

MEASUREMENTS OF NO IN TURBULENT NON-PREMIXED FLAMES STABILIZED ON A BLUFF BODY

B. B. DALLY AND A. R. MASRI

*Department of Mechanical and Mechatronic Engineering
The University of Sydney
NSW 2006, Australia*

R. S. BARLOW AND G. J. FIECHTNER

*Combustion Research Facility
Sandia National Laboratories
Livermore, CA 94551, USA*

D. F. FLETCHER

*Department of Chemical Engineering
The University of Sydney
NSW 2006, Australia*

Spontaneous, single-point measurements of nitric oxide, NO, are made jointly with temperature, OH, and the major species using the Raman/Rayleigh/LIF technique. Turbulent non-premixed flames stabilized on a bluff body are studied with fuels ranging from simple H_2/CO to complex H_2/CH_4 and gaseous methanol. The fuel jet velocity is varied to investigate the Damköhler number effects on the formation of NO. Data are presented for different axial and radial locations along the full length of most flames. It is found that the NO is generated either in the recirculation zone or further downstream of the neck zone. When the stoichiometric contour lies within the outer vortex, NO is produced mainly within the recirculation zone. Within the neck zone of the flame, the NO index levels are either constant or decreasing. This is due to the lower production of NO and the higher contribution of the consumption mechanisms such as NO reburn to N_2 . The overall NO emission level in flames of CH_3OH fuel is about a quarter of that measured in H_2/CO and H_2/CH_4 flames.

Introduction

Growing environmental concerns have led regulatory authorities to impose much stricter control on emissions from combustion systems. This in turn has led to renewed research interests in polluting species such as NO_x , SO_x , and CO. NO_x emission, in particular, has attracted special attention because of its contribution to acid rain and depletion potential of the stratospheric ozone layer. A summary of the emission regulations and control of combustion-generated nitrogen oxide can be found elsewhere [1]. The main constituents of NO_x are NO and NO_2 gases. NO is formed first in all the diffusion-type flames, while NO_2 is a by-product and forms at temperatures in the range of 700–800K. The fraction of NO that converts into NO_2 is believed to be very sensitive to fluid mechanical mixing and basically to the rapid cooling of NO [2]. NO emission from flames is thought to be controlled by four different mechanisms: thermal, prompt, nitrous, and NO re-

burn mechanisms. The relative contribution of each of these mechanisms depends on the fuel type, temperature, pressure, and residence times [3,4].

There have been many experimental studies in turbulent jet diffusion flames investigating the effects of fuel type, Reynolds number, Damköhler number (Da), and radiation heat loss on NO_x formation [4–11]. Bilger and Beck [5] found a shift in the NO peak toward the rich zone and a dependence on the jet exit Reynolds number, $Re^{-1/2}$. Drake et al. [6] suggested that the rich shift of the NO peak is due to probe sampling effects and that the super-equilibrium (O) radical concentration leads to higher NO_x formation rate covering a broader mixture fraction on both lean and rich sides of stoichiometric. Driscoll et al. [7] studied the dependence of the NO_x -emission index ($EINO_x$) on Re and Da numbers and proposed alternate correlations. Turns et al. [8,9] looked at the effects of radiation losses on NO formation and found them to be significant even in nonsooting flames.

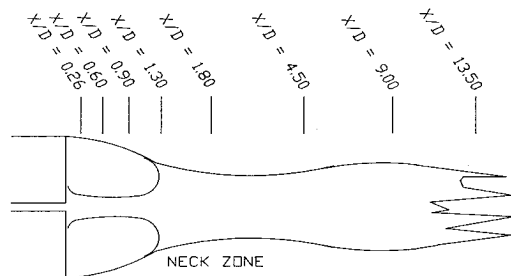


FIG. 1. Sketch of a typical bluff-body-stabilized flame and the measurement locations.

In all of these investigations, the experimental results were mostly obtained using a water-cooled sampling probe positioned downstream of the visible flame tip. These data were used mainly to calculate the NO_x-emission index (EINO_x) normalized by a global residence time that is generally defined, using the similarity assumption, as the length of the flame divided by the bulk jet velocity. This technique suffers from averaging effects and falls short of giving details on the effects of turbulence-chemistry interaction on NO_x and the instantaneous relation between NO concentration and other scalars. Barlow and Carter [12,13] recently have used laser-induced fluorescence (LIF) to make instantaneous and quantitative measurements of NO jointly with temperature and other species using the Raman/Rayleigh/LIF technique. The measurements were made in a H₂ flame diluted with helium. They demonstrated that peak NO occurs at stoichiometric levels and that the rich shift detected by others [5,7] is due to averaging effects. Such nonintrusive and spontaneous measurements of NO in flames are very revealing and extremely important for understanding the evolution of NO in flames.

Fewer attempts have been made to model NO_x formation in turbulent diffusion flames using realistic chemistry. Such efforts must account for all the relevant NO_x-formation mechanisms. This involves many species and reactions and necessitates the use of reduced mechanisms such as those produced recently by Hewson and Williams [4]. A further complication associated with the computation of NO_x is the need to account for the effects of radiation heat losses. Smith et al. [14] recently have tackled such problems using the PDF and CMC approaches for jet diffusion flames with H₂/He fuel.

The purpose of this paper is to present instantaneous measurements of NO jointly with temperature, mixture fraction, and the hydroxyl radical OH in turbulent diffusion flames stabilized on a bluff body. Such measurements are made using the same Raman/Rayleigh/LIF technique used by Barlow and Carter [12]. The novelty here is threefold. First, fuels with complex chemical kinetics such as methanol

and methane are used. Second, the flow pattern is more complex and includes a recirculation zone of fluid just downstream of the jet exit plane. Third, a detailed map of the flame structure is obtained from the recirculation zone to the flame tip. Bluff-body-stabilized flames are of significant practical importance and are being studied extensively. They present an immense challenge to modelers of turbulent combustion.

Experimental Setup

The bluff-body burner has an outer diameter of 50 mm with a concentric jet diameter of 3.6 mm. The wind tunnel has an exit cross section of 254 × 254 mm. The co-flow air velocity is fixed at 40 m/s for all the flames and the free stream turbulence level in the tunnel is at ~2%. The single-point Raman/Rayleigh/LIF technique is used to measure temperature and the concentration of stable species as well as the concentration of two minor species: OH and NO. Figure 1 shows a schematic of the flame and the corresponding measurement locations. The Raman/Rayleigh measurements use two Nd:YAG lasers in which the successive pulses are stretched from ~8 to ~40 ns to avoid excessive energy in the probe volume and hence gas breakdown. The energy delivered to the probe volume is ~700 mJ. The combined Nd:YAG (532-nm) beams are reflected back through the probe volume using a collimating lens and a 180° turning prism, which effectively doubles the Raman and Rayleigh energy to ~1.4 J.

The OH and NO fluorescence measurements are accomplished using two separate Nd:YAG-pumped dye laser systems. The OH excitation beam is tuned for the O₁₂(8) transition in the A²Σ⁺ - X²Π(1, 0) band (λ = 287.9 nm), and the OH signal is collected through broadband colored glass filters, Schott WG-295 and Hoya U-340 (both 3 mm thick). This allows the capture of the fluorescence in both the (1, 0) and (0, 0) band. The NO excitation beam has a wavelength of 225.9 nm, and the signal is collected from the system of bands at 236, 247, 259, and 271 nm. The Raman and Rayleigh scattered light is collected using a six-element achromat and later focused onto the entrance slit of a 0.75-m polychromator. The OH and NO signals are collected using a Cassegrain mirror at the opposite side of the test section from the Raman/Rayleigh lens. A dichroic beam splitter directed the NO fluorescence onto one detector, while the OH fluorescence passed through to another detector. Calibration for the Rayleigh, OH, and the Raman species is done using a laminar premixed flame established on a Hencken burner. A premixed CH₄/air flame stabilized on a McKenna burner is used for the NO calibration. The quantitative OH and NO concentrations are obtained by correcting the

TABLE 1

U_j is the jet velocity (m/s), U_{CO} is the co-flow air velocity (m/s), Re_j is the jet Reynolds number, % BO is the percentage ratio of jet velocity over the blow-off velocity, and T_{IN} is the temperature of the fuel at the jet exit plane

Flame	Symbol	U_j/U_{CO}	Re_j	% BO	T_{IN} (K)
CH ₃ OH	ML1	80/40	23,700	55	373
CH ₃ OH	ML2	121/40	35,900	84	373
H ₂ /CO (2:1)	HC1	134/40	17,500	22	298
H ₂ /CO (2:1)	HC2	321/40	41,990	53	298
H ₂ /CH ₄ (1:1)	HM1	118/40	15,800	50	298
H ₂ /CH ₄ (1:1)	HM2	178/40	23,900	75	298
H ₂ /CH ₄ (1:1)	HM3	214/40	28,700	91	298

fluorescence signals on a shot-to-shot basis for the variations in the Boltzmann fraction and the collisional quenching rate that are determined from the measured temperature and species concentration. Quenching cross sections of NO and OH are obtained from Paul [16–18]. These procedures are described in detail by Barlow and Carter [12].

Three different fuels are investigated: CH₃OH, H₂/CO (2:1), and CH₄/H₂ (1:1) by volume. The first and second fuels have a stoichiometric mixture fraction of 0.135, while the third has a stoichiometry of 0.050. Methanol is evaporated and delivered through heated line before being released at 100°C from the jet. A list of the flames investigated is given in Table 1. The fuel jet velocity is varied to investigate the Damköhler number effect on NO_x formation. The measurements are taken at different axial locations in the flame. Typically, 800 shots are collected at each radial location covering the whole width of the flame.

Results and Discussion

The bluff-body-stabilized flames investigated here are characterized by three distinct zones, shown schematically in Fig. 1. The first is referred to as the recirculation zone. It establishes downstream of the bluff body and extends to ~ 1.0 bluff-body diameter. It has an outer larger vortex close to the air side and, depending on the flow, an inner vortex adjacent to the central jet [15]. Generally, the outer vortex has a nearly uniform mixture and its strength depends on the fuel and flow conditions. The stoichiometric mixture fraction contour is found to shift from the outer vortex to the inner vortex with increasing jet velocity. Beyond the recirculation zone is the neck zone, which is a region of intense mixing in which local extinction and blow off occur at high enough jet velocity. The third zone is the rest of the flame, which spreads in a jetlike manner.

Although detailed measurements have been made in all the flames listed in Table 1, results are only

presented here for flames of methanol fuel. The detailed data for the rest of the fuels will appear elsewhere [19]. Scatter plots of temperature, NO, and OH mole fractions versus the mixture fraction are shown in Fig. 2 for flames ML1 and ML2. Each of these plots corresponds to a different axial location. In flame ML1, the peak NO mole fraction drops from 50 to 20 ppm as the axial location increases from $X/D_B = 0.26$ to 1.8. Further downstream and outside the neck zone ($X/D_B > 1.8$), the flame slows down and the NO peak increases back to ~ 40 ppm. Flame ML2 shows a similar trend for NO, albeit with lower peak values that generally are due to higher jet velocity and hence shorter residence time. Unlike OH concentrations that decrease to zero for mixture fractions greater than ~ 0.25 , the measured NO profile covers almost the entire mixture fraction range. Peak temperature and OH levels in flame ML1 are similar right across the flame length, except at $X/D_B = 0.26$, where lower peak OH is observed. Flame ML2, which is closer to blow off, shows significant local extinction in the neck zone at $X/D_B = 1.6$ with full reignition occurring further downstream at $X/D_B = 4.5$. The intense mixing at the neck zone leads to temperature depression, lower residence time, and hence a decrease in the production of NO. The lower peak NO near stoichiometric is also due to the rapid mixing of NO away from these regions. Peak temperature, OH, and NO occur around stoichiometric for both flames. The average length of these flames, determined as the location at which the average value of the mixture fraction on the centerline reaches the stoichiometric value, is about 9 bluff body diameters, which is much shorter than the visible length.

NO Index

The emission index E_{INO_x} is a nondimensional quantity often used when comparing the NO_x emission from different fuels. Since NO₂ is not measured here and since the measurements cover the whole

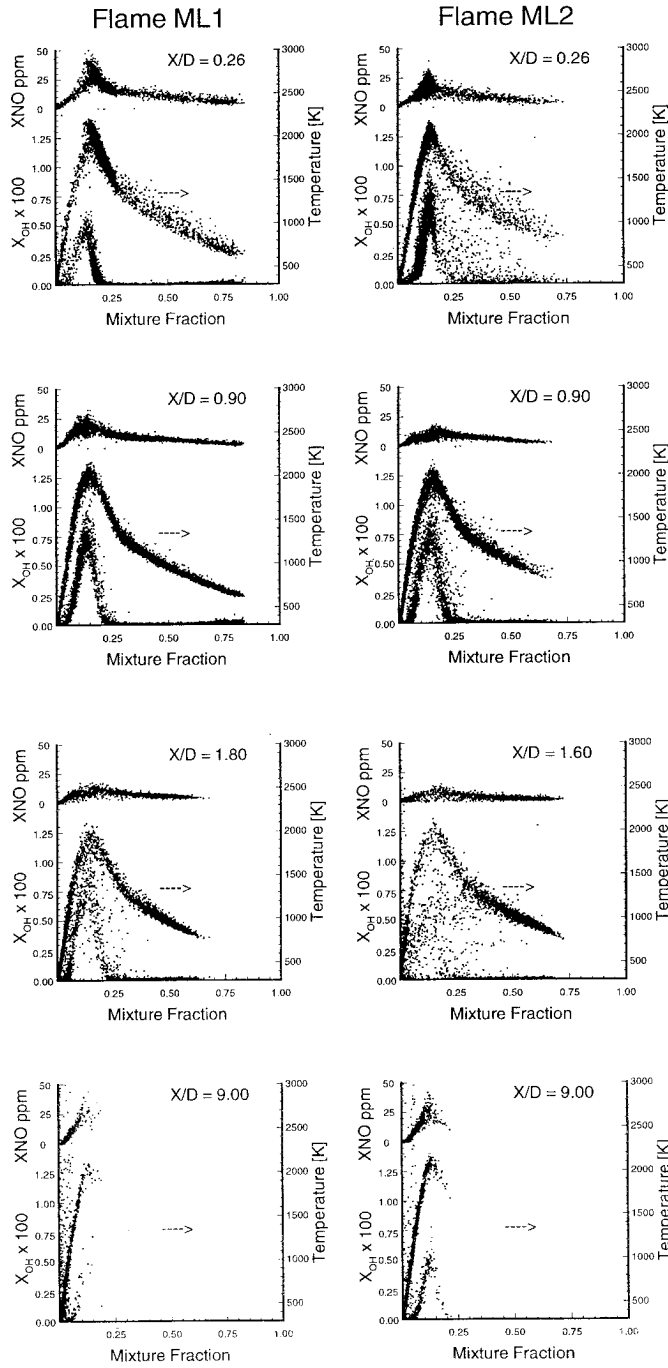


FIG. 2. Scatter plots of temperature and the mole fractions of NO and OH plotted versus mixture fraction for a range of axial locations in the CH₃OH flame with $U_f/U_{BO} = 0.55$ (ML1) and $U_f/U_{BO} = 0.84$ (ML2).

flame length rather than just one location downstream of the tip, a new NO index (NOI) is defined as the net mass of NO convected downstream at a given axial location in the flame per unit mass of jet fuel:

$$NOI = \frac{2\pi W_{NO}}{A\dot{m}_{JET}} \int_0^\infty [N_{NO}(r)]U(r)rdr \quad (1)$$

where W_{NO} is the molecular weight of NO, A is Avogadro's number, \dot{m}_{JET} is the mass flow rate of the

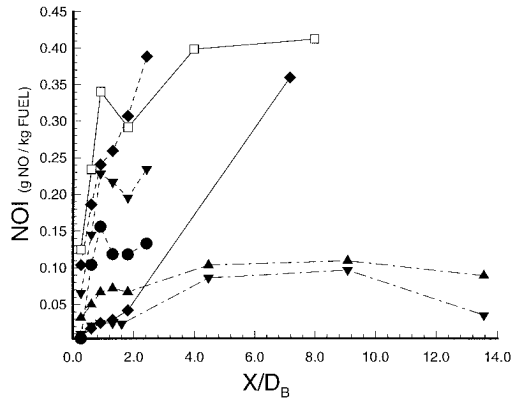


FIG. 3. Axial plot of the NO index (NOI) obtained for bluff-body-stabilized flames with a range of fuels: ---◆--- H_2/CH_4 fuel with $U_j/U_{BO} = 0.50$ (HM1); ---▼--- H_2/CH_4 fuel with $U_j/U_{BO} = 0.75$ (HM2); ---●--- H_2/CH_4 fuel with $U_j/U_{BO} = 0.91$ (HM3); ---□--- H_2/CO fuel with $U_j/U_{BO} = 0.22$ (HC1); ---◆--- H_2/CO fuel with $U_j/U_{BO} = 0.53$ (HC2); ---▲--- CH_3OH fuel with $U_j/U_{BO} = 0.55$ (ML1); ---▼--- CH_3OH fuel with $U_j/U_{BO} = 0.84$ (ML2)

fuel, $[N_{\text{NO}}(r)]$ is the measured mean number density of NO, and $U(r)$ is the computed mean axial velocity at radial location (r). The calculated velocities are used here because measurements are not available at all the axial locations of interest. The flow field is calculated using the CFDS-FLOW3D package [20]. The modified $k-\epsilon$ turbulence model and the “mixed is burnt” combustion model are used in the calculations. More information about these calculations is provided in Ref. [21].

At each axial location, the net mass flow rate of NO is normalized by the fuel mass flow rate at the jet exit plane. Figure 3 shows the NOI for all flames listed in Table 1, plotted against the normalized distance above the burner. It should be noted here that although this index is an approximation (since it uses the mean values of the measured NO concentration and computed velocity), it reveals valuable information about the NO formation or destruction at different locations in the flame. In the H_2/CH_4

flames, measurements are presented down to $X/D_B = 2.4$ only, while the entire flame length is covered for the H_2/CO and CH_3OH fuels. The general trend observed for all flames is an increase in NOI in the recirculation zone followed by a region in the neck zone in which NOI decreases or remains constant. NOI then increases further to a maximum that occurs well downstream of the neck zone. The decrease in NOI at the tip of the methanol flames ML1 and ML2 is largely due to conversion of NO to NO_2 . The decrease in NOI observed at the neck zone of the H_2/CO and H_2/CH_4 flames suggests that the production of NO has dropped considerably and that NO reburn to N_2 , which is enhanced by the combination of a short residence time and high concentration of NO, may be active. The NOI decrease at the neck zone is smaller for lower jet velocity flames.

The following points should be noted:

1. Methanol fuel is a lower NO pollutant with peak NOI being about a quarter that of H_2/CH_4 and H_2/CO fuel mixtures.
2. As the jet velocity is increased and blow off approaches, the NOI level decreases right across the flame, especially in the neck zone where the temperature decreases and local extinction occurs. This is illustrated clearly in the H_2/CO and H_2/CH_4 flames. Further downstream of the neck zone, NOI levels increase again because of reignition and relaxed turbulent mixing rates.
3. The increase in the NOI within the recirculation zone is controlled by the location of the stoichiometric contour with respect to the stabilizing vortices. The vortices' shape and strength are determined by the geometry and jet momentum. At high jet momentum, the outer vortex is shortened and the inner vortex disappears because of the jet expansion. As a consequence, the residence time inside this inner zone is much shorter than in the outer vortex and hence a smaller amount of NO is produced. This implies that for flows in which stoichiometric mixtures are largely within the inner zone, the levels of NO produced in the recirculation zone will be much lower. This is the case for flames HC2 and ML2. The calculations of the flow field [15,21], described above, show

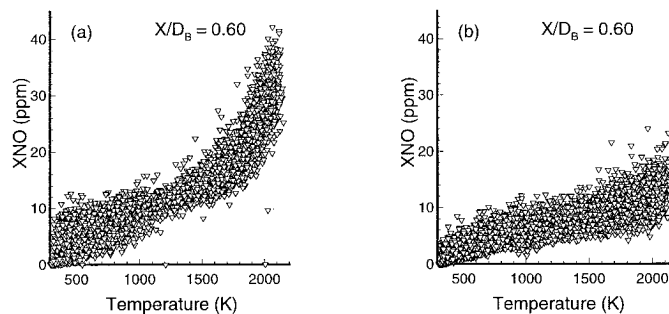


FIG. 4. Scatter plots of NO mole fraction plotted versus temperature at axial location $X/D_B = 0.60$ in flames (a) ML1 and (b) ML2.

that for these flames, the stoichiometric contours are within the inner zone. However, in the H₂/CH₄ flames and the low-velocity HC1 and ML1 flames, the stoichiometric contours are within the outer vortex and hence the levels of NOI within the recirculation zone are much higher.

Analysis of the relative contribution of the various mechanisms to the overall production of NO is beyond the scope of this paper. It is known, however, that this is affected by a range of factors including temperature, residence time, and species concentrations in the radical pool. Figure 4 shows scatter plots of NO mole fraction versus temperature measured at $X/D_B = 0.6$ in the recirculation zones of flames ML1 and ML2. The correlation between NO and temperature changes as the jet velocity is increased and the stoichiometric contour shifts from the outer vortex to the inner zone. The lower peak mole fraction of NO measured in flame ML2 reflects the shorter residence time experienced at this location in the flame. Further analysis of the correlations between temperature, NO, OH, and other scalars coupled with calculations of flames with similar fuel mixtures and detailed or reduced kinetics will be useful in determining the sources of NO.

Conclusions

Single-point measurements of NO made in bluff-body-stabilized flames indicate that peak levels of NO occur at stoichiometric mixture fraction regardless of the fuel mixture, the Damköhler number of the flame, and the axial location in the flame. As the residence time decreases, the correlation between temperature and NO changes, reflecting the lower levels of NO produced. The amount of NO produced in the recirculation zone is very high if the stoichiometric contour lies within the outer vortex and decreases sharply if the stoichiometric contour moves to the inner zone. Within the neck zone of the flame, NOI levels are either constant or decrease because of temperature depression and the low residence time, which decreases the production of NO and increases the contribution of the consumption mechanisms such as the NO return to N₂. The overall NO emission level in flames of CH₃OH fuel is about quarter of that measured in H₂/CO and H₂/CH₄ flames.

Acknowledgments

The authors acknowledge the support of the Australian Research Council and the U.S. Department of Energy, Office of Basic Energy Sciences, Division of Chemical Sciences.

REFERENCES

1. Bowman C. T., *Twenty-Fourth Symposium (International) on Combustion*, The Combustion Institute, Pittsburgh, 1992, pp. 859–878.
2. Hori, M., *Twenty-First Symposium (International) on Combustion*, The Combustion Institute, Pittsburgh, 1986, pp. 1181–1188.
3. Fenimore, C. P., *Thirteenth Symposium (International) on Combustion*, The Combustion Institute, Pittsburgh, 1971, pp. 373–380.
4. Hewson, J. C. and Williams, F. A., *Proceedings of the 8th ONR Propulsion Meeting*, La Jolla, CA, 1995, pp. 52–59.
5. Bilger, R. W. and Beck R. E., *Sixteenth Symposium (International) on Combustion*, The Combustion Institute, Pittsburgh, 1976, pp. 541–551.
6. Drake, M. C., Correa, S. M., Pitz, R. W., Shyy, W., and Fenimore, C. P., *Combust. Flame* 69:347–365 (1987).
7. Driscoll, J. F., Chen, R. H., and Yoon, Y., *Combust. Flame* 88:37–49 (1992).
8. Turns, S. R. and Myhr, F. H., *Combust. Flame* 87:319–335 (1991).
9. Turns, S. R., Myhr, F. H., Bandaru, R. V., and Maund, E. R., *Combust. Flame* 93:255–269 (1993).
10. Chen, R.-H. and Driscoll, J. F., *Twenty-Third Symposium (International) on Combustion*, The Combustion Institute, Pittsburgh, 1990, pp. 281–288.
11. Correa, S. M., *Combust. Sci. Technol.* 87:329–362 (1993).
12. Barlow, R. S. and Carter, C. D., *Combust. Flame* 97:261–280 (1994).
13. Barlow, R. S. and Carter, C. D., *Combust. Flame* (in press).
14. Smith, N. S. A., Bilger, R. W., Carter, C. D., Barlow, R. S., and Chen, J.-Y., *Combust. Sci. Technol.* 105(4,6):357–375 (1995).
15. Dally, B. B., Masri, A. R., and Fletcher, D. F., *Twelfth Australasian Fluid Mechanics Conference*, Vol. 1, Sydney, Australia, 1995, pp. 529–532.
16. Paul, P. H., *J. Quant. Spectrosc. Radiat. Transfer* 51:511–524 (1994).
17. Paul, P. H., Gray, J. A., Durant, J. L. Jr., and Thoman, J. W. Jr., *AIAA J.* 32:1670–1675 (1994).
18. Paul, P. H., Private communication on quenching of OH and NO by methanol; Sandia National Laboratories, Livermore, CA, 1995.
19. Dally, B. B., Masri, A. R., Barlow, R. S., and Fiechtner, G. J., Submitted to *Combust. Flame* (1996).
20. CFDS-FLOW3D release 3.3: user manual; Computational Fluid Dynamics Services, AEA Technology, Harwell Laboratory, Didcot, Oxon, UK, 1995.
21. Dally, B. B., Fletcher, D. F., and Masri, A. R., *Proc. First Asian CFD Conference*, Hong Kong, 1995, pp. 177–182.

COMMENTS

J. P. Gore, Purdue University, USA. Would you comment on the effects of neglecting the cross correlation between NO number density and axial velocity? What is your justification for calculating the emission index without considering this effect?

Author's Reply. The effects of the correlation between NO number density and the velocity are not known and require a joint instantaneous measurement of these scalars. This has not been done and forms an interesting and challenging project. The NOI presented here is an approximate measure of the NO flux which serves as a basis for comparison of the evolution of NO in flames with similar flow field structure and different fuels.

•

A. Ghoniem, MIT, USA. Previous experiments by Namazian et al [1] and by Roquemore et al [2] showed the presence of strong oscillations near the bluff body over a wide range of velocity ratios. Numerical simulations by Martins and Ghoniem [3] and others have shown that these oscillations are related to vortex sheddings and interactions within the recirculation zone, 1–2 bluff-body diameters. Have you detected similar oscillations in your experiments and can strain related effects near the jet flame base be used to interpret some of your observations.

REFERENCES

1. Namazian, M., Kelly, J. T., and Schafer, R. W., *Twenty-Second Symposium (International) on Combustion*, The Combustion Institute, Pittsburgh, 1988, pp. 627–634.
2. Roquemore, W. M., Britton, R. L., and Sandhu, S. S., "Investigation of the dynamic behavior of a bluff-body diffusion flame using flame emission," AIAA-82-0178, AIAA 20th Aerospace Sciences Meeting.
3. Martins, L. T. and Ghoniem, A. F., *ASME J. Fluids Eng.* 115:474–484 (1993).

Author's Reply. The flames investigated in this paper are stable and do not exhibit the oscillations or the vortex shedding referred to in the question. This is mainly due to the fact that the jet and the coflow momentum and hence the Reynolds numbers of these flames are higher than those for the flames referred to by Prof. Ghoniem. For example the Schefer/Namazian methane flame has a coflow and fuel jet momentum of 750 and 300 (N/m²) respectively, as opposed to 1920 and 5200 (N/m²) for the CH₄/H₂ flames presented in this paper. The corresponding Reynolds number is 7000 for the Schefer/Namazian flame and 16,000 and above for the flames discussed in this paper.

